Mon. Not. R. Astron. Soc. **355,** 1272–1282 (2004) doi:10.1111/j.1365-2966.2004.08412.x

Photometric distances to dark clouds: cometary globule CG 12

G. Maheswar,★ P. Manoj★ and H. C. Bhatt★
Indian Institute of Astrophysics, Sarjapur Road, Koramangala, Bangalore 560034, India

Accepted 2004 September 10. Received 2004 September 10; in original form 2004 July 8

ABSTRACT

A method for determining distances to dark clouds and Bok globules based on broad-band optical and near-infrared photometry is presented. In this method, intrinsic colour indices of stars projected towards the direction of a cloud are computed by dereddening the observed colour indices using various trial values of extinction A_V and a standard extinction law. The computed intrinsic colour indices for a star are then compared with the intrinsic colour indices of normal main-sequence stars and a spectral type is assigned to the star for which the computed colour indices best match the standard intrinsic colour indices. Distances (d) to the stars are determined using the A_V and absolute magnitudes (M_V) corresponding to the spectral types thus obtained. A plot of A_V against d undergoes a sharp rise at a distance corresponding to the distance to the cloud. Using this method, we have determined a distance of 550 pc to the cometary globule CG 12. The distance of 550 pc and a Galactic latitude of $b = 21^\circ$ imply that CG 12 is at a height of $\sim$200 pc above the galactic mid-plane. The star formation efficiency in this cloud is found to be relatively high ($\gtrsim$16 per cent, to as large as $\sim$33 per cent). The existence of an H I shell centred at $l = 315^\circ$, $b = 30^\circ$ with CG 12 near its boundary and its tail pointing away from the centre of the shell supports the suggestion of a supernova explosion, near the centre of the H I shell, being responsible for the cometary morphology and the triggering of star formation. Thus CG 12 is a rare example of triggered high-mass star formation at relatively large galactic height.

Key words: stars: distances – stars: formation – ISM: clouds – dust, extinction – ISM: globules – ISM: individual: CG 12.

1 INTRODUCTION

Small dark clouds or globules are the natural places to look for isolated star formation (Bok & Reilly 1947). Bok globules are probably the nearest and simplest structures in the interstellar medium. Optically they appear as dark, roundish patches against the stellar background and have well-defined edges and high extinctions.

As for any astronomical object, the measurement of distance to an interstellar cloud is very important. Distances to interstellar clouds are needed in order to determine several important physical properties like sizes, masses and densities (Clemens, Yun & Heyer 1991). Distances are also needed for obtaining luminosities of any embedded young stellar objects or protostars in these clouds (Yun & Clemens 1990).

The traditional method of determining distances to interstellar clouds utilizes star counts (Bok & Bok 1941) or Wolf diagrams (Wolf 1923), which plot the number of stars versus apparent magnitude. However, the distance determination using these methods depends on questionable extrapolations of luminosity functions in order to work for small clouds. The other methods which have generally been used to determine the distance of interstellar clouds are: photometry (usually *UBVRI* or Strömgren); distances of stars or fields associated with a cloud; kinematic distances from CO velocities; geometric distances from the galactic coordinates, using the empirical formula of Herbst & Sawyer (1981); *D*-line absorption spectra of Na I; and polarized light from the background stars. An additional method of assigning distances to small dark clouds involves bracketing the cloud distance by using spectroscopic distances to stars close in front of and behind the cloud to infer the cloud distance (Hobbs, Blitz & Magnani 1986). For a better estimate of distance to interstellar clouds, it is essential to have spectroscopic data for sufficient number of stars in front of and behind the cloud, which is not only tedious but also requires lot of observing time. Using broad-band photometry and identifying unreddened M dwarfs in front of and reddened M dwarf stars behind the cloud from $(B - V)$ versus $(V - I)$ plots, one can bracket the cloud and determine its distance (Peterson & Clemens 1998). But finding M dwarfs both just in front of and behind the cloud is extremely difficult, especially for small nearby clouds.

In this paper, we present a method to find distances to interstellar clouds using broad-band *VRIJHK* photometry of stars in the field

★E-mail: maheswar@iiap.ernet.in; hcbhatt@iiap.ernet.in; manoj@iiap.ernet.in

containing the cloud. The method has been described and demonstrated using observations of the fields containing the cometary globule CG 12. In Section 2, we describe the method used to estimate the distance to interstellar clouds. Observations and data analysis performed for CG 12 are discussed in Section 3. Results and discussions are presented in Section 4. In Section 5, we summarize the results obtained in this paper.

2 THE METHOD

The photometric (in the V band, say) distance (d) to a star is given by

$$\log d = (V - M_V + 5 - A_V)/5, \quad (1)$$

where V, M_V and A_V are apparent magnitude, absolute magnitude and extinction, respectively. The distance can be determined if we know M_V and A_V. The absolute magnitude depends on the spectral type of the star. The spectral type also determines various colours $(V - R)$, $(V - I)$, $(V - J)$, $(V - H)$, $(V - K)$ etc. The observed colours are generally reddened due to interstellar extinction, which is wavelength-dependent. By assuming a value for A_V and the extinction law (considered here to be the mean interstellar extinction law and the same for all the stars), one can estimate the various colour excesses and correct the observed colours to find the intrinsic colours of the stars. The computed intrinsic colours are then compared with the standard unreddened intrinsic colours of normal stars to determine the spectral type and hence a value for M_V. Various trial values of A_V are used and a star is assigned a spectral type for which the computed colour indices best match (χ^2 minimum) with the standard intrinsic colour indices.

The method of determining distances to dark clouds involves five steps. First, we measure the observed V, R, I, J, H and K magnitudes of the stars in the field containing the cloud. Second, we find the intrinsic colour indices $(V - R)_\mathrm{i}$, $(V - I)_\mathrm{i}$, $(V - J)_\mathrm{i}$, $(V - H)_\mathrm{i}$ and $(V - K)_\mathrm{i}$ of each star from the equations (2–6) obtained assuming: (i) a normal interstellar extinction law (ratio of total-to-selective extinction, $R_V = 3.1$; Mathis 1990); and (ii) that stars are in their main-sequence evolutionary stages. The equations relating the observed and dereddened colours are

$$(V - R)_\mathrm{i} = (V - R)_\mathrm{o} - 0.252A_V, \quad (2)$$

$$(V - I)_\mathrm{i} = (V - I)_\mathrm{o} - 0.518A_V, \quad (3)$$

$$(V - J)_\mathrm{i} = (V - J)_\mathrm{o} - 0.718A_V, \quad (4)$$

$$(V - H)_\mathrm{i} = (V - H)_\mathrm{o} - 0.825A_V, \quad (5)$$

$$(V - K)_\mathrm{i} = (V - K)_\mathrm{o} - 0.888A_V, \quad (6)$$

where $(V - R)_\mathrm{o}$, $(V - I)_\mathrm{o}$, $(V - J)_\mathrm{o}$, $(V - H)_\mathrm{o}$ and $(V - K)_\mathrm{o}$ are the observed colour indices and A_V is the interstellar extinction in the visual band, which is an unknown parameter in the above equations. Various trial values of A_V are used. For the illustrative case of CG 12, a set of values of A_V was used ranging from 0 to 6 in steps of 0.1 mag. These equations provide 60 sets of intrinsic colour indices for each star with each set corresponding to one value of A_V. Thirdly, we compare each of these 60 sets of intrinsic colour indices obtained for each star with the intrinsic colour indices for main-sequence stars of different spectral types. The main-sequence colour indices $(V - R)_\mathrm{ms}$ and $(V - I)_\mathrm{ms}$ are taken from Johnson (1966) and $(V - J)_\mathrm{ms}$, $(V - H)_\mathrm{ms}$ and$(V - K)_\mathrm{ms}$ are taken from Koornneef (1983). One of the intrinsic colour indices among the 60 sets obtained for a star matches best with the intrinsic colour indices for a main-sequence star of a particular spectral type, giving a minimum value of χ^2 defined as

$$\chi^2 = \sum_\lambda \frac{[(V - \lambda)_\mathrm{i} - (V - \lambda)_\mathrm{ms}]^2}{(V - \lambda)^2_\mathrm{ms}},$$

where $\lambda \equiv R$, I, J, H and K. This method provides not only the spectral type for each star in the field but also the extinction towards it. Fourthly, the distance to each star can be obtained by using equation (1), where values of M_V corresponding to the assigned spectral types are obtained from the absolute magnitude versus spectral type calibration (Schmidt-Kaler 1982). Fifthly, the distance to the cloud is taken to be that value where, in a plot of extinction against distance to the star, the extinction increases steeply above the normal galactic extinction towards that direction. We have used this method to obtain the distance to the cometary globule CG 12 as described below.

3 COMETARY GLOBULE CG 12: DISTANCE DETERMINATION

Cometary globule CG 12 is an isolated globule at a relatively large galactic latitude ($l = 316.5^\circ, b = 21.2^\circ$) associated with the reflection nebula NGC 5367 surrounding the double star h4636 in its head. It was first identified as a cometary globule by Hawarden & Brand (1976) on an ESO/SRC Sky Survey plate taken with the UK Schmidt telescope. Its head is ∼10 arcmin in diameter, and its nebular tail is more than 1° in length and is oriented nearly perpendicular to the galactic plane. Optical polarimetric observations of stars towards CG12 showed the magnetic field lines in this region to be roughly parallel to the cometary tail (Marraco & Forte 1978; Bhatt, Maheswar & Manoj 2004) of the globule. CG 12 has been detected in CO (van Till, Loren & Davis 1975; White 1993; Yonekura et al. 1999; Otrupcek, Hartley & Wang 2000) and in dense ($>10^3$ cm^{-3}) gas tracers like H_2CO (Goss et al. 1980) and NH_3 (Bourke, Hyland & Robinson 1995) molecular-line observations. The CO and *IRAS* study of CG 12 by White (1993) revealed the presence of a bipolar molecular outflow centred close to the IRAS 13547-3944 source and the double star h4636. They found the outflow to be well collimated and roughly parallel to the direction of the tail. Santos et al. (1998) showed the presence of a couple of objects, in their near-infrared images of a region around IRAS 13546-3941 in CG 12, with near-infrared colours characteristic of low-mass young stellar objects. This evidence show that star formation is currently taking place in CG 12. The double-star system h4636 consists of two B-type stars (B4 + B7), both showing near-infrared excess, and the northern B4 component, also showing Hα in emission (Williams et al. 1977; Maheswar, Manoj & Bhatt 2002). CG 12 is thus an example of a high galactic latitude cloud undergoing current star formation.

The relatively high galactic latitude position ($b \simeq 21^\circ$) of CG 12 could be due to two reasons. Either it is at a distance closer than ∼200 pc, adopting a scaleheight $\langle z \rangle$ of ∼60 pc above the galactic mid-plane for the clouds in the solar vicinity (Magnani, Blitz & Mundy 1985; Keto & Myers 1986), or it is farther away and at a relatively large galactic height. Keto & Myers (1986), based on the assumption that the molecular gas is in hydrostatic equilibrium with the external gravitational field produced by stars near the galactic plane, estimated a mean expected distance $\langle d \rangle$ for a sample of southern high-latitude clouds and adopted this value ($\langle d \rangle = 100$ pc) for the distance to CG 12. van Till et al. (1975), in order to estimate the mass of CG 12 from CO observations, assigned a distance of

300 pc, assuming a value of 200 pc for the thickness of the galactic hydrogen gas layer in the solar vicinity and assuming that CG 12 is at the upper limit of the range suggested by its galactic latitude. Using 300 pc as the distance, they estimated the mass of CG 12 to be $\sim$30 $M_\odot$. Bourke et al. (1995) assigned a distance of 400 pc to CG 12, assuming it to be associated with the cometary globules in the Vela–Gum nebula region. From *UBV* photometry of a set of 11 stars projected towards CG 12, which includes stars associated with nebulosities within the cloud, Williams et al. (1977) determined a distance of 630 pc. Marraco & Forte (1978) estimated a distance of 660 pc based on the observed β index and (β, M_V) calibration of a single star, star 2 (as numbered in Williams et al. 1977). Thus there exists a range (100–660 pc) of distances for CG 12 in the literature. The most favoured distance to CG 12 is 630 pc estimated by Williams et al. (1977) because this distance estimate is based on stars of which some are associated with the cloud. The method assumes the stars to be on the zero-age main sequence (ZAMS). However, the stars with nebulosities and infrared excesses are likely to be young and pre-main-sequence objects. Thus absolute magnitudes, the character of reddening caused by the circumstellar dust around these stars and the distances derived should be considered uncertain. Uncertainty in the distance to the cloud leads to uncertainties in various derived physical parameters. For example, the cloud mass derived from the measured gas column density scales with the square of the distance. The star formation efficiency [SFE = mass of the stars formed/(mass of the stars + mass of the cloud)] will scale roughly inversely with the square of the distance if the stellar masses are derived from spectral types. The height of the cloud above the galactic plane scales linearly with distance. If CG 12 is a nearby cloud (with distance $<$200 pc, say), then this will be a low-mass cloud with high SFE. On the other hand, if it is as distant as $\sim$600 pc, then it is a massive cloud at a large ($\sim$200 pc) height above the galactic plane undergoing star formation with a lower SFE. In this case CG12 would be one of those rare clouds forming early-type stars at relatively large galactic heights ($\sim$200 pc as compared with the typical scaleheight of $\lesssim$65 pc for B-type stars; Reed 2000). Therefore, a determination of distance to CG 12 is important in order to find its true location in the galaxy and to study the process of star formation at high galactic latitudes. We have made CCD photometric and spectroscopic observations of CG 12 and determined its distance following the method described in Section 2.

3.1 Observations and data analysis

Both photometric and spectroscopic observations of CG 12 were carried out with the 2.34-m Vainu Bappu Telescope (VBT) at the Vainu Bappu Observatory, Kavalur, India.

3.1.1 Spectroscopy

Optical CCD spectra of 11 stars were obtained using the OMR (Optomechanics Research) spectrograph (Prabhu, Anupama & Surendiranath 1998) on the VBT during the period 2001–2004. Photometric studies of these 11 stars which are projected towards the head region of CG 12 had earlier been carried out by Williams et al. (1977). All spectra were obtained with a slit of 2 arcsec width and spectral resolution of 1.3 –2.6 Å pixel^{-1}. All spectra were bias-subtracted, flat-field corrected, extracted and wavelength-calibrated in the standard manner using the IRAF reduction package. Spectral types were determined for the stars by comparing the observed spectrum with those in the atlas of Jacoby, Hunter & Christian (1984).

3.1.2 Optical photometry

Images of CG 12 centred at two positions (2000 coordinates), $13^h57^m35^s - 39^\circ54'19''$ (Region I) and $13^h57^m43^s - 40^\circ00'54''$ (Region II) were carried out on 2003 April 24 and 2004 February 2004, respectively, at the prime focus ($f/3.23$) of VBT using a Tektronix CCD chip (Roper Scientific, Tucson, AZ, USA) of size 1024×1024 pixel^2. The observed fields (each covering 10.75×10.75 arcmin^2 of the sky) are shown in Fig. 1 as Region I and Region II. Also marked and numbered in Fig. 1 are stars studied by Williams et al. (1977). Images were taken in *BVRI* filters. Typical seeing during the observations was $\sim$2.5 arcsec. During each observing run, twilight flats were acquired in all the filters. The bias frames were obtained at regular intervals. The bias frames closer to the observed image were used for bias subtraction. The flat frames were first bias-subtracted before stacking (using median) to obtain master flats for each filter. These master flats are used to flat-field the images. The star detection algorithm DAOFIND in IRAF was used to get the positions of the stars in the images. The aperture photometry was performed on the stars in the images using APPHOT in IRAF. Star 4 in Williams et al. (1977) was used to transform the observed fluxes to magnitudes. Observations of this star through *B* and *V* filters exist for three different epochs. The observed magnitudes in *B* and *V* filters are: 10.15 and 9.15 from Marraco & Forte (1978); 10.15 and 9.13 from Williams et al. (1977); and 10.06 and 9.13 from the Tycho-2 catalogue (Hog et al. 2000). This shows that this star is not a photometric variable (within the observational errors) and can therefore be used to transform observed fluxes to magnitudes. The uncertainties in the derived magnitudes are generally $\sim$0.05 mag. The images taken through the B filter were not deep enough and hence were not considered in further analysis. The processed CCD images of the fields containing CG 12 through *V*, *R* and *I* filters are shown in Fig. 2. Figs 2(a), (b) and (c) show CCD images of Region I through *V*, *R* and *I* filters, respectively; Figs 2(d), (e) and (f) show CCD images of Region II through *V*, *R* and *I* filters, respectively.

3.1.3 2MASS near-infrared measurements

Near-infrared JHK_s magnitudes for the stars in both the frames were obtained from the The Two Micron All Sky Survey (2MASS; Cutri et al. 2000) catalogue. To ensure high-quality data, a maximum uncertainty of 0.1 mag was permitted in all three bands. The JHK_s colours were transformed from the 2MASS system to the Koornneef system using the relations given by Carpenter (2001).

4 RESULTS AND DISCUSSION

4.1 Distance to CG 12

A total of 143 stars from Region I and Region II are selected and the photometric results are presented in Tables 1 and 2, respectively. The 11 stars studied by Williams et al. (1977) (shown and identified in Fig. 1), of which some are associated with nebulosities and have near-infrared excesses and hence could be pre-main-sequence stars, are excluded from the current analysis. In both Tables 1 and 2, columns 1, 2 and 3 are self-explanatory. Columns 4–9 give photometric magnitudes and corresponding errors in *V*, *R* and *I* filters from our observations. Columns 10–15 give photometric magnitudes and corresponding errors in *J*, *H* and *K* filters obtained from 2MASS observations. Columns 16–18 give A_V, χ^2 and spectral type obtained from the method described in Section 2. Column 19 gives absolute magnitudes (M_V) for the corresponding spectral types and column 20 gives the estimated distances to the stars using equation (1). The

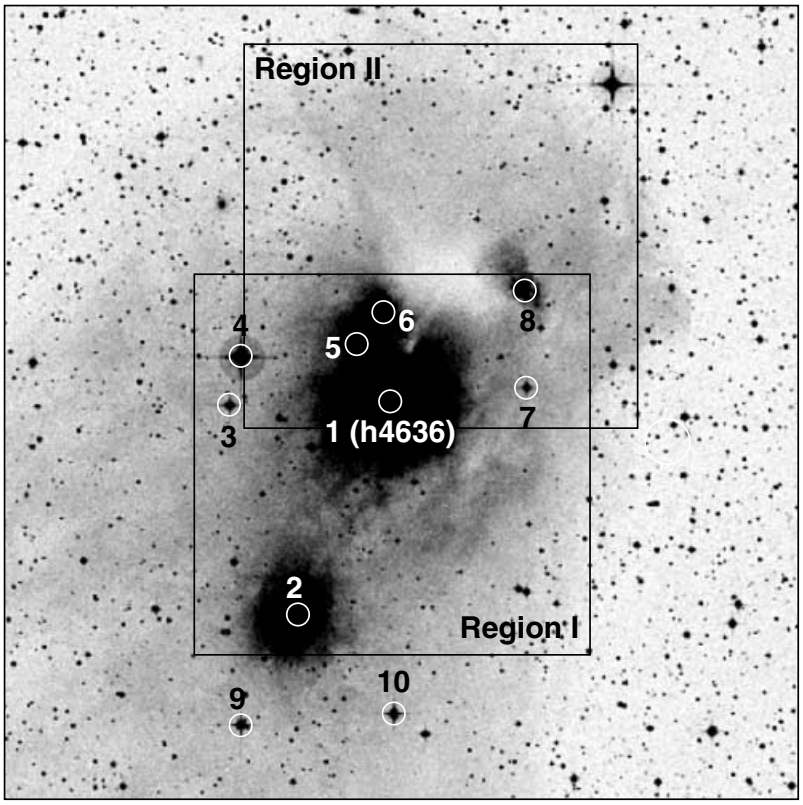

Figure 1. Regions I & II, observed to measure photometric magnitudes of stars projected towards CG 12, are shown on this 20 × 20 arcmin^2 Digitized Sky Survey (DSS) image. North is up and east is to the left. Also numbered are stars studied by Williams et al. (1977).

estimated distance (d) and A_V of stars projected towards CG 12 are plotted in Fig. 3. Our stars for which $\chi^2 \lesssim 0.1$ are used in the plot. We have separated the stars observed into two groups depending on whether they are within or outside the cloud boundary [judged visually from Digitized Sky Survey (DSS) images]. In Fig. 3, filled and open circles represent stars found projected within and outside the cloud boundary, respectively. In order to understand the global variation of extinction in the direction of CG 12, we have also considered other stars within a radius of 5° of CG 12 for which spectral information is known from the literature. B and V magnitudes of these stars were taken from the Tycho-2 catalogue (Hog et al. 2000). Distances and extinction for these stars were estimated and overplotted in Fig. 3, represented by open squares. The solid line represents the galactic obscuration as a function of distance (d) at a galactic latitude of 21° obtained from the expression given by Bahcall & Soneira (1980). They have assumed an exponential variation of the density of obscuring layer with height above the galactic plane.

Examination of Fig. 1 shows that the reflecting material in CG 12 is not distributed uniformly and lacks sharp boundary, unlike in some of the dark globules such as Barnard 68 (Bok 1977). Therefore the increase in A_V with distance, even for stars projected within the cloud boundary, is not expected to take a step-like jump at the distance of CG 12. Extinction towards stars projected outside the cloud boundary is found to increase slowly with distance, but is generally $\lesssim$0.7 mag even for distances as large as ∼1 kpc. These stars represent the behaviour of extinction due to the general interstellar medium in the direction. It can be seen from Fig. 3 that most of the stars that show extinction values much larger than expected due to the general interstellar medium are at distances $\gtrsim$550 pc. This (550 pc) is also the distance at which a distinct jump in extinction appears, although a few stars at ∼400 pc show unusually large values of extinction ($A_V \gtrsim 2$ mag). As discussed in Section 4.2, for stars showing large values of A_V, the reddening law could be anomalous and their derived distances would be less reliable. We therefore disregard these stars and ascribe the sharp rise in extinction at ∼550 pc to the presence of the cloud CG 12 at this distance. The star with $A_V \approx 1$ mag and distance ≈ 200 pc in Fig. 3 shows an unusually large extinction for its derived distance. This star could be a red giant behind the cloud. Its observed colours are equally well fitted ($\chi^2 = 0.0590$ as compared to the $\chi^2 = 0.0602$ for a fit with main-sequence K5 spectral type) by a reddened K4 giant with $A_V \sim 0.7$ mag at a distance of ∼7 kpc. This and other possible errors and uncertainties in the distance determination using this method are discussed in Section 4.2.

Photometry in UBV for 11 stars projected towards the head region of CG 12 was performed by Williams et al. (1977). From the two-colour diagram they concluded that most of the stars are reddened variously. A colour–magnitude diagram from $(B - V)_o$ and V_o found by tracing the stars back along standard reddening vectors in two-colour diagram was drawn and a ZAMS with a distance modulus of 9 mag was fitted to the stars illuminating the nebulosity. From their study, stars 2, 7 and 8 and both components of h4636 fall on the ZAMS. They assumed stars 5 and 6 to be pre-main-sequence and star 4 to be an unreddened foreground star. Marraco & Forte (1978) assigned a spectral type of B6V and an absolute magnitude M_V of +0.2 to star 2 by means of observed β index and (β, M_V) calibration. They derived a distance of 660 pc to CG 12, assuming $R_V = 3$. We have estimated distances to these stars by determining their spectral types from the observed spectra.

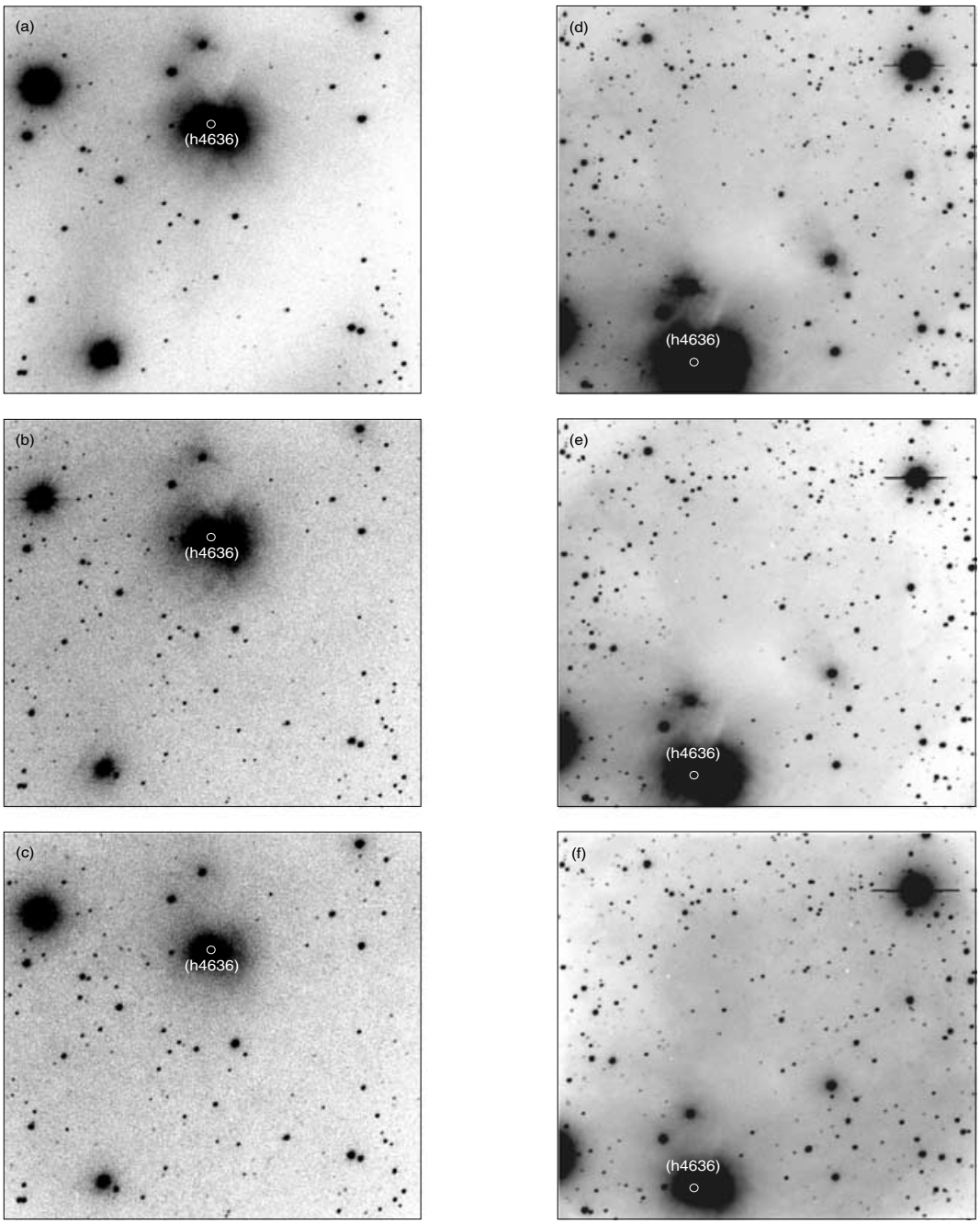

Figure 2. CCD images of the observed fields shown in Fig. 1. North is up and east is to the left. Panels (a), (b) and (c) are CCD images of Region I in V, R and I filters, respectively, and figures (d), (e) and (f) are CCD images of Region II in V, R and I filters, respectively. All the CCD images cover a 10.75×10.75 arcmin^2 area each on the sky. The brightest star h4636 (star 1 in Williams et al. 1977), surrounded by nebulosity, is marked on each image.

Our spectroscopic results for the 11 stars studied photometrically by Williams et al. (1977) are given in Table 3. Column 1 gives star numbers as given by Williams et al. (1977). 1N and 1S represent northern and southern components of h4636 respectively. Columns 2 and 6 give observed magnitudes in V-band and $(B - V)$ values taken from Williams et al. (1977), respectively. Column 3 gives spectral types determined by comparing the observed spectrum with those in the atlas of Jacoby et al. (1984). The spectral types determined by us and that estimated by Williams et al. (1977) from the two-colour diagram are in good agreement with each other except for star 5. We have observed a spectral type of G9 for star 5, whereas they have assigned a spectral type of A4 to it. Columns 4 and 5 give corresponding intrinsic colour index and absolute magnitude, respectively. Columns 7, 8 and 13 give estimated colour excess, A_V $[= 3.1\ E(B - V)]$ and distance to the stars. Near-infrared colour indices (JHK magnitudes are from 2MASS observations) are given in columns 9 and 11, with colour excesses in columns 10 and 12.

The distances and A_V for the 11 stars are overplotted in Fig. 3, represented by unfilled star symbols. Extinction towards stars 3, 4, 5 and 10 is $\lesssim 0.5$ and their distances are 501, 417, 204 and 427 pc, respectively. Stars 2, 6, 8 and h4636 are clearly associated with CG 12 because there exist reflection nebulosities around them.

Table 1. Photometric results for stars in Region I.

Star number (1)	RA (°) (2000) (2)	Dec. (°) (2000) (3)	V (4)	ϵ_V (5)	R (6)	ϵ_R (7)	I (8)	ϵ_I (9)	J (10)	ϵ_J (11)	H (12)	ϵ_H (13)	K (14)	ϵ_K (15)	A_V (16)	χ^2 (17)	Sp (18)	M_V (19)	d (pc) (20)
1	209.335	−39.925	17.15	0.03	16.32	0.04	15.20	0.03	14.51	0.03	13.85	0.03	13.58	0.04	0.4	0.0846	K5	7.4	743
2	209.343	−40.005	19.06	0.07	17.75	0.06	16.95	0.05	15.49	0.07	14.71	0.07	14.33	0.08	1.6	0.0717	K5	7.4	1030
3	209.346	−40.055	17.30	0.04	16.26	0.03	15.08	0.03	14.22	0.03	13.63	0.03	13.39	0.04	1.0	0.0471	K5	7.4	603
4	209.350	−40.045	16.05	0.03	15.41	0.03	14.77	0.03	14.24	0.03	13.68	0.03	13.53	0.05	0.2	0.0454	K2	6.4	779
5	209.357	−40.034	15.55	0.02	14.87	0.02	14.32	0.02	13.81	0.03	13.21	0.02	13.08	0.03	0.2	0.0235	K2	6.4	617
6	209.363	−40.061	13.22	0.02	12.35	0.02	11.50	0.02	10.46	0.02	9.72	0.03	9.45	0.02	0.4	0.0966	K5	7.4	121
7	209.369	−40.084	17.85	0.04	16.55	0.04	15.02	0.03	13.75	0.03	13.10	0.02	12.79	0.03	2.2	0.0823	K5	7.4	448
8	209.376	−40.060	18.99	0.06	17.88	0.06	17.07	0.05	15.76	0.07	15.15	0.08	14.65	0.09	1.1	0.0766	K5	7.4	1253
9	209.376	−40.042	18.54	0.05	17.47	0.05	16.31	0.04	15.14	0.04	14.30	0.05	13.97	0.05	1.4	0.1041	K5	7.4	888
10	209.390	−40.093	18.16	0.05	17.08	0.04	16.46	0.04	15.52	0.05	14.86	0.07	14.85	0.13	0.4	0.0119	K5	7.4	1185
11	209.410	−40.069	18.43	0.05	17.61	0.05	17.12	0.06	16.24	0.11	15.70	0.15	15.64	0.22	0.6	0.0304	K2	6.4	1934
12	209.414	−40.021	17.16	0.03	16.14	0.03	15.14	0.03	14.38	0.03	13.70	0.02	13.61	0.04	0.6	0.0229	K5	7.4	680
13	209.415	−40.069	18.23	0.05	17.31	0.05	16.21	0.04	15.54	0.05	14.73	0.05	14.70	0.11	0.6	0.0544	K5	7.4	1114
14	209.417	−40.093	19.04	0.06	17.54	0.05	16.77	0.05	15.92	0.07	15.12	0.10	14.87	0.12	1.2	0.0209	K7	7.8	1020
15	209.417	−40.057	18.19	0.05	16.86	0.04	15.67	0.03	14.50	0.02	13.73	0.04	13.53	0.04	2.1	0.0226	K4	7.0	660
16	209.423	−40.086	18.35	0.05	17.09	0.04	16.09	0.04	15.84	0.07	15.29	0.10	14.98	0.15	0.1	0.0024	M0	8.8	777
17	209.444	−40.046	17.34	0.04	16.24	0.03	15.50	0.03	14.52	0.03	13.91	0.04	13.65	0.04	1.5	0.0114	K2	6.4	773
18	209.446	−40.016	16.86	0.03	16.00	0.03	15.27	0.03	14.49	0.04	13.91	0.03	13.79	0.05	0.9	0.0256	K2	6.4	820
19	209.451	−40.020	16.45	0.03	15.70	0.03	15.04	0.03	14.36	0.02	13.82	0.04	13.75	0.05	0.5	0.0330	K2	6.4	814
20	209.452	−40.038	19.20	0.07	17.89	0.06	16.97	0.05	16.01	0.08	15.10	0.09	15.08	0.14	1.3	0.0063	K5	7.4	1264
21	209.453	−40.067	17.02	0.03	15.80	0.03	15.02	0.03	14.04	0.03	13.29	0.02	13.11	0.03	1.5	0.0079	K3	6.7	582
22	209.454	−40.011	16.61	0.03	15.61	0.03	14.77	0.03	13.72	0.03	12.98	0.03	12.77	0.03	0.7	0.0537	K5	7.4	504
23	209.456	−40.027	16.93	0.03	16.12	0.03	15.36	0.03	14.54	0.03	13.97	0.04	13.75	0.05	0.9	0.0575	K2	6.4	845
24	209.460	−40.039	18.11	0.05	17.30	0.05	16.58	0.05	15.50	0.06	15.13	0.08	14.83	0.12	0.4	0.0799	K4	7.0	1391
25	209.462	−39.984	17.92	0.04	17.00	0.04	16.22	0.04	15.25	0.05	14.64	0.06	14.33	0.10	1.3	0.0593	K2	6.4	1109
26	209.464	−40.078	16.81	0.03	15.69	0.03	14.97	0.03	14.27	0.04	13.72	0.04	13.58	0.05	0.2	0.0027	K6	7.6	636
27	209.469	−40.093	17.49	0.04	16.54	0.04	15.85	0.04	15.17	0.05	14.63	0.05	14.30	0.09	0.3	0.0050	K4	7.0	1091
28	209.476	−40.002	13.32	0.02	12.85	0.02	12.50	0.02	12.26	0.02	11.88	0.02	11.87	0.02	0.0	0.0195	G2	4.7	531
29	209.485	−40.011	17.84	0.04	16.52	0.04	15.07	0.03	13.99	0.03	13.35	0.03	12.98	0.03	2.0	0.0439	K5	7.4	488
30	209.490	−39.963	17.99	0.04	16.98	0.04	16.27	0.04	15.50	0.06	14.84	0.06	14.64	0.10	1.2	0.0031	K2	6.4	1199
31	209.490	−39.990	16.23	0.03	15.53	0.03	14.56	0.03	14.22	0.04	13.61	0.04	13.33	0.05	0.0	0.0780	K4	7.0	703
32	209.493	−40.013	18.18	0.05	16.90	0.04	15.71	0.04	14.54	0.04	13.68	0.03	13.31	0.04	2.0	0.0473	K4	7.0	687
33	209.494	−39.998	16.08	0.03	15.24	0.03	14.52	0.03	13.66	0.03	13.05	0.03	12.82	0.03	0.3	0.0424	K4	7.0	571
34	209.500	−40.037	19.44	0.08	18.14	0.06	17.22	0.06	16.09	0.09	15.38	0.10	15.09	0.14	2.3	0.0109	K2	6.4	1408
35	209.501	−40.051	18.56	0.05	17.37	0.05	16.36	0.04	15.25	0.05	14.64	0.06	14.26	0.08	1.5	0.0254	K4	7.0	1029
36	209.502	−40.090	15.58	0.02	14.71	0.02	13.95	0.02	13.21	0.03	12.70	0.03	12.57	0.03	0.0	0.0181	K5	7.4	434
37	209.502	−40.021	15.23	0.02	14.32	0.02	13.69	0.02	13.08	0.03	12.46	0.03	12.32	0.03	0.2	0.0023	K4	7.0	404
38	209.502	−39.951	16.29	0.03	15.56	0.03	14.92	0.03	14.37	0.03	13.85	0.04	13.77	0.05	0.4	0.0251	K2	6.4	793
39	209.512	−39.981	17.30	0.04	16.33	0.04	15.68	0.03	14.87	0.03	14.45	0.06	14.11	0.06	1.0	0.0063	K2	6.4	957
40	209.518	−40.050	14.00	0.02	13.31	0.02	12.84	0.02	12.46	0.02	11.92	0.03	11.86	0.03	0.2	0.0055	K1	6.1	347
41	209.521	−40.040	17.99	0.04	16.99	0.04	16.28	0.04	15.63	0.06	15.21	0.08	14.81	0.12	0.4	0.0048	K4	7.0	1316
42	209.522	−39.979	18.60	0.06	17.63	0.05	16.44	0.04	15.84	0.08	15.17	0.09	15.00	0.13	0.7	0.0515	K5	7.4	1260
43	209.522	−40.073	15.85	0.02	15.09	0.03	14.42	0.03	13.74	0.02	13.33	0.03	13.10	0.03	0.5	0.0287	K2	6.4	619
44	209.524	−39.993	18.94	0.06	17.23	0.05	16.41	0.04	14.99	0.04	14.09	0.04	13.78	0.05	2.3	0.0542	K5	7.4	707
45	209.525	−40.004	18.08	0.05	16.63	0.04	15.59	0.03	14.63	0.04	13.98	0.04	13.80	0.06	1.5	0.0045	K6	7.6	627
46	209.527	−40.031	18.30	0.05	17.30	0.05	16.62	0.05	15.37	0.05	14.71	0.06	14.79	0.12	0.6	0.0667	K5	7.4	1151
47	209.529	−39.997	18.10	0.05	17.34	0.05	16.29	0.04	15.59	0.06	15.01	0.08	14.89	0.12	0.2	0.0890	K5	7.4	1260
48	209.533	−40.060	17.53	0.04	16.41	0.04	15.39	0.03	14.37	0.03	13.61	0.03	13.27	0.04	1.4	0.0379	K4	7.0	670
49	209.536	−40.085	18.18	0.05	16.93	0.04	15.63	0.03	15.03	0.04	14.47	0.05	14.01	0.06	1.1	0.0215	K7	7.8	720
50	209.537	−39.964	16.23	0.03	15.53	0.03	14.91	0.03	14.48	0.03	13.89	0.04	13.83	0.05	0.4	0.0219	K1	6.1	886
51	209.538	−40.066	18.33	0.05	17.28	0.05	16.02	0.04	15.44	0.05	14.71	0.07	14.44	0.08	0.8	0.0478	K6	7.6	970
52	209.541	−40.089	17.36	0.04	16.57	0.04	15.81	0.04	15.16	0.04	14.56	0.05	14.50	0.09	0.7	0.0338	K2	6.4	1131
53	209.320	−40.002	16.78	0.03	16.19	0.03	15.58	0.03	15.10	0.04	14.61	0.05	14.61	0.10	0.0	0.0496	K2	6.4	1192
54	209.321	−40.058	17.27	0.04	16.73	0.04	16.01	0.04	15.67	0.08	14.94	0.09	15.06	0.15	0.0	0.1022	K2	6.4	1494
55	209.324	−40.024	15.43	0.02	14.86	0.02	14.37	0.03	13.89	0.03	13.45	0.03	13.42	0.04	0.0	0.0388	K1	6.1	737
56	209.326	−40.040	16.13	0.03	15.48	0.03	14.95	0.03	14.37	0.03	13.81	0.04	13.71	0.05	0.1	0.0288	K2	6.4	845
57	209.339	−40.082	16.64	0.03	16.25	0.03	15.76	0.04	15.62	0.07	15.30	0.11	15.21	0.16	0.0	0.0741	G1	4.6	2562
58	209.342	−40.079	17.24	0.04	16.11	0.03	14.82	0.03	13.85	0.03	13.38	0.03	13.06	0.03	1.3	0.0533	K5	7.4	512
59	209.342	−40.038	17.78	0.04	17.04	0.04	16.36	0.04	15.58	0.06	14.81	0.06	14.80	0.10	0.1	0.0654	K4	7.0	1369
60	209.343	−40.057	17.87	0.04	16.88	0.04	15.79	0.04	15.04	0.05	14.35	0.05	14.22	0.07	0.7	0.0387	K5	7.4	900
61	209.347	−40.052	17.58	0.04	16.80	0.04	16.13	0.04	15.44	0.07	14.88	0.08	14.77	0.12	0.0	0.0240	K4	7.0	1307
62	209.377	−40.089	16.79	0.03	16.19	0.03	15.57	0.03	14.96	0.04	14.307	0.04	14.35	0.08	0.2	0.0808	K2	6.4	1093

Table 2. Photometric results for stars in Region II.

Star number (1)	RA (°) (2000) (2)	Dec. (°) (2000) (3)	V (4)	ϵ_V (5)	R (6)	ϵ_R (7)	I (8)	ϵ_I (9)	J (10)	ϵ_J (11)	H (12)	ϵ_H (13)	K (14)	ϵ_K (15)	A_V (16)	χ^2 (17)	Sp (18)	M_V (19)	d (pc) (20)
1	209.311	−39.975	19.00	0.03	17.66	0.02	15.98	0.01	14.82	0.04	14.17	0.04	14.01	0.07	2.4	0.0888	K5	7.4	709
2	209.315	−39.898	13.43	0.01	12.81	0.01	12.35	0.01	11.76	0.02	11.37	0.02	11.26	0.02	0.0	0.0337	K2	6.4	255
3	209.321	−39.953	17.47	0.02	16.32	0.02	15.19	0.01	14.01	0.03	13.19	0.02	12.87	0.03	1.5	0.0725	K5	7.4	530
4	209.333	−39.902	16.86	0.02	16.01	0.01	15.37	0.01	14.65	0.04	14.03	0.05	13.85	0.05	0.2	0.0165	K4	7.0	849
5	209.335	−39.925	17.40	0.02	16.36	0.02	15.36	0.01	14.51	0.03	13.85	0.03	13.58	0.04	0.8	0.0262	K5	7.4	711
6	209.335	−39.877	17.71	0.02	16.62	0.02	15.52	0.01	14.60	0.03	14.05	0.04	13.75	0.06	1.0	0.0311	K5	7.4	748
7	209.347	−39.905	17.47	0.02	16.79	0.02	16.12	0.01	15.33	0.05	14.88	0.06	14.53	0.09	0.0	0.0717	K4	7.0	1234
8	209.350	−39.952	14.89	0.01	14.31	0.01	13.88	0.01	13.40	0.03	12.96	0.02	12.86	0.03	0.0	0.0341	K1	6.1	566
9	209.350	−39.875	17.20	0.02	16.55	0.02	15.97	0.01	15.32	0.06	14.93	0.09	14.75	0.10	0.2	0.0405	K2	6.4	1323
10	209.360	−39.947	19.84	0.04	18.22	0.03	17.16	0.02	15.40	0.06	14.48	0.05	13.98	0.06	2.8	0.0940	K5	7.4	869
11	209.361	−39.911	18.25	0.02	17.31	0.02	16.51	0.02	15.53	0.07	14.87	0.06	14.56	0.10	0.4	0.0522	K5	7.4	1260
12	209.370	−39.883	17.07	0.02	16.30	0.02	15.63	0.02	15.57	0.06	14.89	0.07	14.75	0.10	0.6	0.0333	K0	5.9	1305
13	209.371	−39.884	17.05	0.02	16.21	0.02	15.44	0.01	14.99	0.04	14.48	0.06	14.22	0.07	1.4	0.0163	G2	4.7	1551
14	209.379	−39.966	19.26	0.03	17.96	0.03	16.93	0.02	15.89	0.08	14.93	0.07	14.72	0.10	1.8	0.0173	K4	7.0	1227
15	209.378	−39.926	20.05	0.04	18.23	0.03	16.33	0.02	14.52	0.04	13.96	0.04	13.57	0.05	4.0	0.0679	K5	7.4	551
16	209.384	−39.977	18.70	0.03	17.30	0.02	15.96	0.01	14.89	0.03	14.24	0.05	13.95	0.06	2.0	0.0173	K5	7.4	742
17	209.385	−39.906	15.31	0.01	14.69	0.01	14.23	0.01	13.70	0.03	13.15	0.03	13.12	0.03	0.0	0.0317	K2	6.4	605
18	209.394	−39.886	18.32	0.02	17.26	0.02	16.19	0.01	15.18	0.05	14.43	0.04	13.98	0.06	1.1	0.0629	K5	7.4	945
19	209.402	−39.956	18.29	0.02	17.12	0.02	15.89	0.01	14.95	0.04	14.45	0.06	14.10	0.07	1.3	0.0330	K5	7.4	850
20	209.400	−39.888	19.96	0.04	18.55	0.03	17.18	0.02	15.81	0.07	15.08	0.08	14.58	0.09	2.4	0.0547	K5	7.4	1102
21	209.408	−39.858	16.59	0.01	15.68	0.01	14.80	0.01	13.76	0.03	13.02	0.03	12.72	0.02	0.6	0.0856	K5	7.4	537
22	209.416	−39.901	18.10	0.02	16.85	0.03	15.45	0.01	14.19	0.03	13.56	0.03	13.28	0.04	2.0	0.0731	K5	7.4	563
23	209.421	−39.868	18.77	0.03	17.48	0.02	16.26	0.02	15.10	0.04	14.50	0.06	14.11	0.06	2.0	0.0307	K4	7.0	891
24	209.435	−39.864	18.66	0.03	17.40	0.02	15.98	0.01	14.93	0.03	14.26	0.06	13.95	0.06	1.9	0.0500	K5	7.4	763
25	209.450	−39.958	12.81	0.01	12.22	0.01	11.81	0.01	11.21	0.02	10.71	0.02	10.62	0.02	0.0	0.0501	K2	6.4	192
26	209.452	−39.872	17.00	0.02	16.01	0.01	15.11	0.01	14.29	0.04	13.55	0.04	13.39	0.04	0.6	0.0280	K5	7.4	647
27	209.458	−39.920	19.20	0.03	17.70	0.02	16.29	0.02	14.91	0.05	13.97	0.04	13.73	0.04	2.6	0.0418	K5	7.4	709
28	209.474	−39.959	20.78	0.06	18.99	0.04	17.29	0.02	15.77	0.08	15.04	0.07	14.63	0.10	3.6	0.0199	K5	7.4	928
29	209.476	−39.923	14.83	0.01	13.80	0.01	12.77	0.01	11.74	0.02	11.02	0.02	10.75	0.02	1.0	0.0602	K5	7.4	198
30	209.482	−39.990	19.55	0.04	17.78	0.02	15.90	0.01	14.33	0.03	13.53	0.03	13.20	0.04	3.8	0.0494	K5	7.4	480
31	209.487	−39.922	14.65	0.01	14.00	0.01	13.45	0.01	12.82	0.02	12.34	0.03	12.19	0.03	0.2	0.0381	K2	6.4	407
32	209.490	−39.990	16.14	0.01	15.26	0.01	14.42	0.01	14.22	0.04	13.61	0.04	13.33	0.05	1.1	0.0263	K0	5.9	675
33	209.490	−39.963	17.66	0.02	16.82	0.02	16.14	0.01	15.50	0.06	14.84	0.06	14.64	0.10	0.1	0.0161	K4	7.0	1285
34	209.493	−39.989	14.50	0.01	13.63	0.01	12.82	0.01	12.01	0.02	11.35	0.03	11.05	0.02	0.2	0.0433	K5	7.4	246
35	209.493	−39.946	19.96	0.04	18.34	0.03	16.59	0.02	15.05	0.04	14.24	0.04	13.93	0.06	3.4	0.0636	K5	7.4	697
36	209.492	−39.911	18.59	0.02	17.51	0.02	16.36	0.02	15.45	0.05	14.65	0.05	14.56	0.09	1.1	0.0441	K5	7.4	1068
37	209.500	−39.931	17.32	0.02	16.05	0.01	14.68	0.01	13.43	0.02	12.68	0.03	12.36	0.02	2.0	0.0687	K5	7.4	393
38	209.502	−39.951	16.12	0.01	15.49	0.01	14.87	0.01	14.37	0.03	13.85	0.04	13.77	0.05	0.1	0.0396	K2	6.4	841
39	209.282	−39.890	13.88	0.01	13.31	0.01	12.81	0.01	12.34	0.02	11.69	0.02	11.66	0.03	0.0	0.0568	K2	6.4	314
40	209.284	−39.877	14.33	0.01	13.84	0.01	13.45	0.01	13.09	0.03	12.63	0.03	12.62	0.03	0.2	0.0467	G2	4.7	770
41	209.288	−39.958	14.97	0.01	14.40	0.01	13.96	0.01	13.59	0.02	13.22	0.03	13.14	0.04	0.3	0.0124	G2	4.7	987
42	209.291	−39.970	15.85	0.01	15.20	0.01	14.70	0.01	14.16	0.03	13.61	0.03	13.54	0.04	0.0	0.0198	K2	6.4	778
43	209.291	−39.953	15.85	0.01	15.30	0.01	14.80	0.01	14.31	0.03	13.84	0.02	13.95	0.06	0.0	0.0550	K1	6.1	880
44	209.292	−39.862	16.34	0.01	15.67	0.01	15.16	0.01	14.60	0.03	13.96	0.03	13.89	0.05	0.1	0.0273	K2	6.4	929
45	209.294	−39.913	14.74	0.01	14.16	0.01	13.68	0.01	13.20	0.02	12.76	0.02	12.64	0.03	0.0	0.0360	K1	6.1	527
46	209.294	−39.889	14.71	0.01	14.24	0.01	13.86	0.01	13.52	0.03	13.12	0.03	13.10	0.03	0.1	0.0328	G2	4.7	963
47	209.297	−39.916	16.54	0.01	15.88	0.02	15.28	0.01	14.64	0.03	14.05	0.04	13.88	0.05	0.0	0.0515	K3	6.7	930
48	209.300	−39.969	14.94	0.01	14.23	0.01	13.65	0.01	13.02	0.02	12.43	0.02	12.32	0.02	0.3	0.0293	K2	6.4	446
49	209.300	−39.860	14.48	0.01	13.99	0.01	13.61	0.01	13.31	0.03	12.94	0.04	12.94	0.04	0.0	0.0162	G3	4.8	849
50	209.304	−39.983	15.30	0.01	14.74	0.01	14.32	0.01	13.94	0.03	13.49	0.03	13.44	0.04	0.3	0.0240	G2	4.7	1152
51	209.303	−39.940	17.74	0.02	16.94	0.02	16.20	0.01	15.50	0.05	14.91	0.06	14.74	0.10	0.2	0.0292	K4	7.0	1274
52	209.310	−39.967	13.55	0.01	13.08	0.01	12.72	0.01	12.47	0.03	12.06	0.02	12.01	0.02	0.0	0.0185	G2	4.7	590
53	209.314	−39.992	16.74	0.01	16.10	0.02	15.59	0.01	15.30	0.06	14.79	0.06	14.70	0.10	0.0	0.0111	K1	6.1	1327
54	209.313	−39.961	15.83	0.01	15.18	0.01	14.56	0.01	13.92	0.03	13.57	0.04	13.37	0.04	0.2	0.0411	K2	6.4	704
55	209.313	−39.833	15.50	0.01	14.92	0.01	14.46	0.01	14.04	0.03	13.54	0.03	13.48	0.04	0.0	0.0270	K1	6.1	750
56	209.313	−39.841	15.85	0.01	15.40	0.01	14.77	0.01	14.63	0.04	14.17	0.05	14.06	0.07	0.0	0.0872	G9	5.7	1081
57	209.314	−39.860	14.17	0.01	13.71	0.01	13.30	0.01	13.03	0.03	12.69	0.03	12.58	0.03	0.0	0.0233	G2	4.7	785
58	209.334	−39.846	16.68	0.01	16.10	0.02	15.67	0.01	15.25	0.05	14.57	0.05	14.66	0.09	0.0	0.0471	K1	6.1	1289
59	209.356	−39.850	16.69	0.01	15.99	0.02	15.45	0.01	14.82	0.04	14.19	0.05	14.15	0.07	0.2	0.0273	K2	6.4	1045
60	209.362	−39.857	17.03	0.02	16.36	0.02	15.81	0.01	15.38	0.06	14.85	0.08	14.67	0.10	0.1	0.0177	K2	6.4	1280
61	209.368	−39.827	17.19	0.02	16.59	0.02	16.07	0.01	15.70	0.06	15.11	0.07	14.86	0.10	0.0	0.0447	K2	6.4	1443
62	209.382	−39.842	17.71	0.02	16.85	0.02	16.19	0.01	15.43	0.05	14.71	0.07	14.71	0.10	0.2	0.0248	K4	7.0	1254

Table 2 – *continued*

Star number (1)	RA (°) (2000) (2)	Dec. (°) (2000) (3)	V (4)	ϵ_V (5)	R (6)	ϵ_R (7)	I (8)	ϵ_I (9)	J (10)	ϵ_J (11)	H (12)	ϵ_H (13)	K (14)	ϵ_K (15)	A_V (16)	χ^2 (17)	Sp (18)	M_V (19)	d (pc) (20)
63	209.389	−39.836	16.78	0.02	16.18	0.02	15.71	0.01	15.19	0.04	14.67	0.05	14.56	0.10	0.0	0.0356	K2	6.4	1195
64	209.414	−39.848	17.03	0.02	16.42	0.02	15.91	0.01	15.28	0.05	14.94	0.07	14.65	0.10	0.0	0.0385	K2	6.4	1341
65	209.422	−39.847	17.83	0.02	16.76	0.02	15.58	0.01	14.74	0.03	13.98	0.03	13.82	0.05	1.1	0.0425	K5	7.4	753
66	209.428	−39.852	16.95	0.02	16.13	0.01	15.47	0.01	14.66	0.04	14.15	0.05	13.92	0.05	0.2	0.0284	K4	7.0	885
67	209.431	−39.853	17.41	0.02	16.44	0.02	15.55	0.01	14.43	0.03	13.65	0.02	13.36	0.04	0.8	0.0900	K5	7.4	712
68	209.431	−39.846	16.94	0.02	16.28	0.02	15.72	0.01	15.18	0.04	14.58	0.07	14.55	0.09	0.2	0.0286	K2	6.4	1172
69	209.442	−39.849	15.52	0.01	14.70	0.02	13.97	0.01	13.09	0.03	12.39	0.03	12.24	0.03	0.1	0.0555	K5	7.4	412
70	209.445	−39.847	17.02	0.02	16.37	0.02	15.73	0.01	15.37	0.05	14.87	0.06	14.73	0.10	0.2	0.0280	K1	6.1	1379
71	209.455	−39.835	13.13	0.01	12.55	0.01	12.13	0.01	11.75	0.03	11.29	0.03	11.16	0.02	0.4	0.0277	G2	4.7	404
72	209.463	−39.890	16.76	0.01	16.13	0.01	15.53	0.01	15.03	0.04	14.53	0.06	14.23	0.08	0.1	0.0424	K2	6.4	1130
73	209.466	−39.877	16.25	0.01	15.54	0.01	14.94	0.01	14.27	0.03	13.71	0.03	13.53	0.04	0.4	0.0377	K2	6.4	778
74	209.467	−39.837	15.52	0.01	15.03	0.01	14.65	0.01	14.43	0.04	13.99	0.03	13.95	0.06	0.0	0.0169	G2	4.7	1460
75	209.470	−39.879	17.02	0.02	16.42	0.02	15.84	0.01	15.28	0.05	14.86	0.06	14.67	0.10	0.0	0.0477	K2	6.4	1331
76	209.475	−39.852	17.40	0.02	16.59	0.02	15.92	0.01	15.20	0.05	14.51	0.05	14.32	0.07	0.1	0.0333	K4	7.0	1138
77	209.481	−39.889	16.74	0.02	16.12	0.01	15.60	0.01	15.24	0.06	14.79	0.06	14.71	0.10	0.0	0.0155	K1	6.1	1327
78	209.485	−39.901	15.15	0.01	14.30	0.01	13.58	0.01	12.67	0.02	11.90	0.03	11.75	0.03	0.2	0.0594	K5	7.4	332
79	209.491	−39.890	14.62	0.01	14.06	0.01	13.61	0.01	13.14	0.02	12.73	0.02	12.66	0.03	0.4	0.0431	G2	4.7	802
80	209.495	−39.894	16.08	0.01	15.52	0.01	15.05	0.01	14.55	0.03	14.22	0.04	14.03	0.07	0.0	0.0441	K1	6.1	980
81	209.498	−39.837	15.99	0.01	15.41	0.01	14.94	0.01	14.68	0.04	14.07	0.04	14.23	0.07	0.3	0.0308	G3	4.8	1480

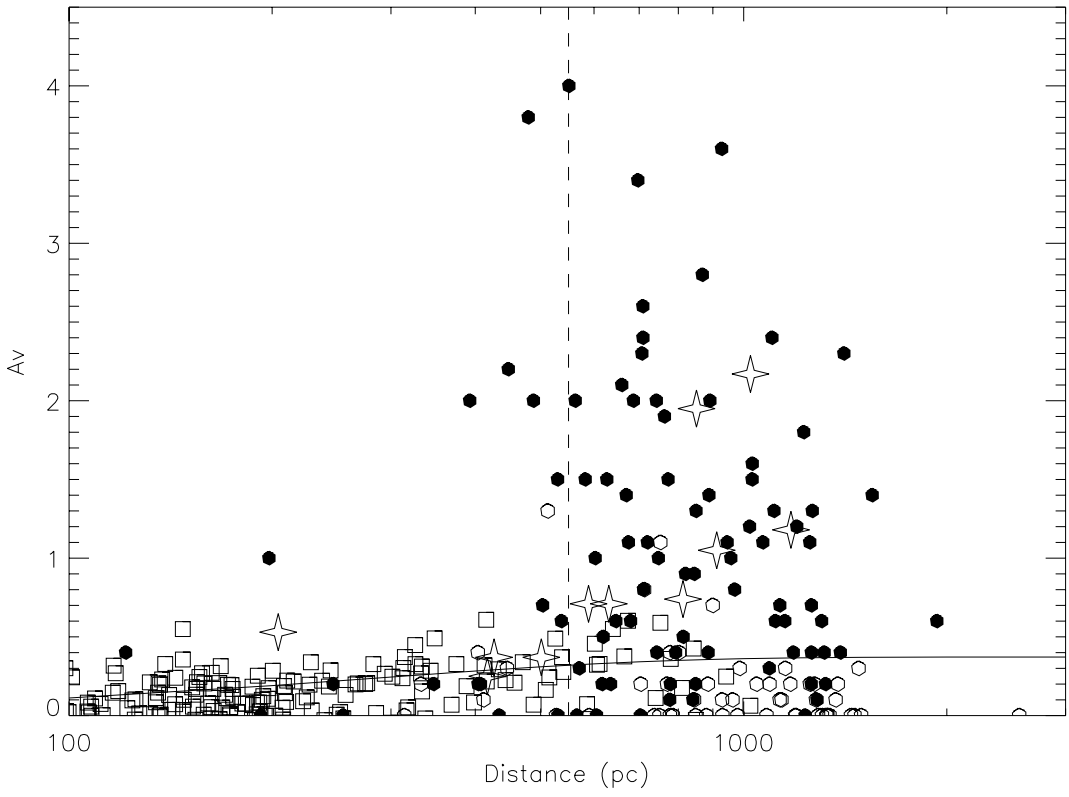

Figure 3. Distance versus A_V plot for stars in Regions I & II using the method described in Section 2. Open stars: stars studied by Williams et al. (1977); filled circles: stars found projected within the cloud boundary; open circles: stars found projected outside the cloud boundary; open squares: stars within a radius of 5° of CG 12 from literature. The solid line represents the galactic obscuration as a function of distance (d) at a galactic latitude of 21° obtained from the expression given by Bahcall & Soneira (1980). The vertical line is drawn at a distance of 550 pc (see Section 4.1 for further explanation).

Extinction values for these stars are $\gtrsim$0.7 mag and they have a wide range of derived distances (∼800–1200 pc). Stars 7 and 9 also have extinction $\gtrsim$0.7 mag and may be also associated with CG 12. Thus for distances $\lesssim$600 pc the extinction is $\lesssim$0.5 but beyond ∼600 pc the extinction increases to $\gtrsim$0.7 mag, similar to that of star 2, which is associated with the cloud.

Based on this partial analysis of 11 stars, one would conclude that the cloud is at a distance of ∼600 pc. However, the derived distances

Table 3. Spectroscopic results on 11 stars studied by Williams et al. (1977).

Object ID	V (mag)	Spectral Type	$(B-V)_o$	M_V	$(B-V)$	$E(B-V)$	A_V	$(J-H)$	$E(J-K)$	$(H-K)$	$E(H-K)$	Distance (pc)
(1)	(2)	(3)	(4)	(5)	(6)	(7)	(8)	(9)	(10)	(11)	(12)	(13)
1N*	10.70	B4	−0.19	−1.5	0.51	0.70	2.17	0.400	0.480	1.077	1.107	1024
1S*	10.26	B7	−0.14	−0.6	0.20	0.34	1.05	0.652	0.682	1.004	1.024	912
2*	10.08	B8	−0.11	−0.2	0.13	0.24	0.74	0.080	0.110	0.078	0.088	813
3	12.45	F6	0.47	3.6	0.59	0.12	0.37	0.371	0.171	−0.024	−0.084	501
4	9.13	G8III†	0.94	0.8	1.02	0.08	0.25	0.425	−0.045	0.215	0.095	417
5	12.77	G9	0.77	5.7	0.94	0.17	0.53	0.492	0.152	0.105	0.005	204
6*	13.30	A4	0.12	1.8	0.50	0.38	1.18	0.387	0.337	0.333	0.323	1175
7	13.31	F4	0.41	3.6	0.64	0.23	0.71	0.344	0.152	0.018	−0.032	631
8*	12.91	A2	0.05	1.3	0.68	0.63	1.95	0.447	0.417	0.261	0.251	851
9	11.96	A9	0.27	2.4	0.50	0.23	0.71	0.220	0.070	−0.004	−0.044	589
10	12.11	F4	0.41	3.6	0.53	0.12	0.37	0.286	0.096	0.030	−0.010	427

†Marraco & Forte (1978) classified star 4 as a G8III on the basis of $V-R$ and $V-I$ colours. * Stars associated with nebulosities.

to stars 2, 6, 8 and h4636 with nebulosities show a wide range. Their distances should be considered very uncertain for various causes discussed below.

4.2 Errors and uncertainties

The main contribution to the errors in deriving distances to stars projected towards a cloud using the method described in Section 2 comes from the following.

4.2.1 Reddening laws

The average value of R_V in our galaxy is found to be 3.1. However, there exist regions of higher extinction where the value of R_V departs from the average value of 3.1 to higher values (Kandori et al. 2003). Stars 2, 6, 8 and h4636, even though they are associated with CG 12, have a larger range in their distances (∼800–1200 pc). In the distance determination, we have used R_V as 3.1. Towards higher obscuration regions, R_V can be as high as 6.0 (Vrba & Rydgren 1984; Whittet et al. 1987; Kandori et al. 2003). Application of a fixed $R_V = 3.1$ can lead to large discrepancies between distances of stars which are clearly associated with the cloud (Thé et al. 1986). Knowing the spectral type of background stars of the clouds, one can estimate R_V from colour excess ratios $R_V = 1.1[E(V-K)/E(B-V)]$ (Whittet 2003). From Table 3, it can be noted that all the five stars have near-infrared excesses that could be due to heated dust in their vicinity. It is well known that infrared excess can lead to spuriously high estimates of R_V, producing additional flux in the K-band which inflates the value of $E(B-V)$. However, by assuming all these five stars to be located at a distance of 550 pc, R_V values independent of infrared excesses can be deduced. R_V values thus derived towards stars 2, 6, 8, h4636N and h4636S are 6.8, 7.4, 4.6, 5.0 and 6.4, respectively. This shows that the value of R_V in CG 12 is anomalous. The regions with $A_V > 2$ can have values of R_V which differ from that of non-star-forming regions (Kandori et al. 2003). Hence results obtained for stars with $A_V > 2$ from our distance method could have large errors and should be viewed cautiously.

4.2.2 Main-sequence intrinsic colours and binarity

The dereddened observed colours are fitted with the intrinsic colours of standard normal main-sequence stars. However, there can be a scatter in their ages within the main-sequence stage itself. This scatter can give errors in estimating the spectral types and hence in distance determination. If a star is in a binary system, then the combined apparent magnitude of the star would be brighter than that of the individual components. This would make the star appear closer than its true distance and can lead to considerable uncertainties at larger distances.

4.2.3 Evolved and pre-main-sequence stars

Because most of the field stars are in the main sequence, we have assumed that the stars are all of luminosity class V and used the corresponding values of M_V. However, a few stars could be evolved objects that have moved away from the main sequence. For example in Fig. 3, as discussed in Section 4.1, the star with $A_V \approx 1$ mag and at a distance of ≈200 pc is found to be consistent with a reddened ($A_V \sim 0.7$) K4 giant. This will place this star behind the cloud at a distance of ∼7 kpc. The presence of objects with near-infrared colours that are characteristic of low-mass young stellar objects (Santos et al. 1998) and the presence of a low-luminosity molecular outflow (White 1993) give evidence for continuing star formation at the present epoch. Hence there could be pre-main-sequence stars in the regions of CG 12. Because giants and pre-main-sequence stars have higher luminosities compared with dwarfs of similar spectral types, if they are wrongly classified as dwarfs then that can lead to shorter distances with higher values of A_V.

4.3 Star formation at high galactic latitudes

The distance of 550 pc to CG 12 implies that it is at a height of ∼200 pc above the galactic mid-plane. The double star h4636 and stars 2, 6 and 8 are associated with nebulosities. They are of spectral types B4 and B7 (the northern and southern components of h4636, respectively), B8, A4 and A2, respectively. Association of early-type stars with nebulosities suggests that they are relatively young. Also, the northern component of h4636 shows Hα in emission and is surrounded by a dust shell (Williams et al. 1977; Maheswar et al. 2002), indicating that it is still embedded and accreting matter. Detection of a couple of near-infrared sources with colours characteristics of young stellar objects (Santos et al. 1998) and discovery of a well-collimated low-luminosity molecular outflow near the infrared object IRAS 13547-3944 (White 1993) indicate ongoing low-mass star formation in CG 12. Thus CG 12 is an example of a cloud forming high-mass (B-type) stars at a galactic height of ∼200 pc in which low-mass star formation is also active. Formation of massive B-type stars at such large galactic heights must be quite rare because

the scaleheight of early B-type stars is only ∼65 pc (Reed 2000). From CO observations, van Till et al. (1975) estimated the mass of CG 12 to be $\sim 30\,M_\odot$ by assigning a distance of 300 pc. Because the cloud mass scales with the square of the distance, using 550 pc for the distance, the mass of CG 12 becomes $\sim 100\,M_\odot$.

The morphology of CG 12 is similar to cometary globules found elsewhere in our galaxy. The largest of such systems of cometary globules is associated with the Gum Nebula in Vela–Puppis, with ∼30 cometary globules (Zealey et al. 1983; Reipurth 1983) centred around the Vela OB2 association. Two alternative scenarios have been proposed to explain the morphology of cometary globules. The first scenario states that relatively smaller dense cores distributed in a parent giant molecular cloud, exposed to the radiation and stellar winds from massive OB-type stars in a newly born central OB association, can develop cometary head–tail morphology as the less dense core is shock-compressed to produce the head. The shocks can also trigger star formation in the CG head (Reipurth 1983). The alternative scenario is for a supernova blast-wave to sweep past a cloud clump, causing the material to compress and stream out, forming the head and the tail, respectively (Brand et al. 1983). At a distance of ∼550 pc CG 12 is fairly isolated, with no luminous OB-type stars that could produce the head–tail morphology of CG 12 with the tail pointing towards the galactic plane. Williams et al. (1977) suggested that a high galactic latitude supernova explosion at $l \simeq 320^\circ$, $b \simeq 30^\circ$ could be the cause of cometary morphology and triggering of star formation. The presence of a shell or loop of H I centred near $l = 320^\circ$, $b = 30^\circ$ in the radiophotograph by Heiles (1976) was proposed as evidence for this. Only a part of this loop is seen in the H I map of Heiles (1976) as their H I observations did not entirely cover the region containing CG 12 due to its southern declination. The H I maps in Cleary, Haslam & Heiles (1979) and Dickey & Lockman (1990) that combine both northern and southern sky surveys in H I do show the presence of a complete H I shell of $\sim 20^\circ$ angular diameter centred near $l = 315^\circ, b = 30^\circ$. CG 12, as seen in projection, is positioned close to the shell boundary and its cometary tail points away from the centre of the H I shell. The supernova theory for the cometary morphology and star formation in CG 12 is therefore plausible. However, it is not clear whether this dense globule was formed as a result of the supernova remnant expanding into the ambient interstellar gas or whether it was a pre-existing cloud.

A lower limit to the total mass of recently formed stars in the cloud can be computed by summing up the masses (corresponding to the main-sequence spectral types) of the stars 1 (h4636, B4+B7), 2 (B8), 6 (A4) and 8 (A2) that are associated with nebulosities involved in the cloud and show characteristics of young stellar objects (YSOs). Using stellar mass values (Schmidt-Kaler 1982) of 6.4, 4.5, 3.8, 2.4 and 2.1 $M_\odot$ for the spectral types B4, B7, B8, A2 and A4, respectively, the total mass M_* of the young stars formed in the cloud is $\gtrsim 19\,M_\odot$. Therefore the SFE [$= M_*/(M_* + M_{\rm gas})$, where $M_{\rm gas}$ ($\sim 100\,M_\odot$) is the mass of the cloud in gas form] is $\gtrsim 16$ per cent. The cloud is also forming stars with masses lower than that of star 6 ($2.1\,M_\odot$), the least massive of the optically visible YSOs. In addition to CO outflow and infrared sources detected by White (1993) and Santos et al. (1998), there could be other as yet undiscovered lower-mass YSOs in CG 12. If the star formation process in CG 12 produces young stars with a mass function similar to the Salpeter initial mass function ($\mathrm{d}n_*/\mathrm{d}m_* \propto m_*^{-2.35}$, where $\mathrm{d}n_*$ is the number of stars in the mass range $m_* + \mathrm{d}m_*$), as also found in many embedded star clusters like Trapezium and IC 348 (Lada & Lada 2003), and stars as low in mass as $0.6\,M_\odot$ (below which the initial mass function seems to flatten and then decline beyond $\sim 0.1\,M_\odot$), then, by integrating the mass function over the range $0.6\,M_\odot$ to $6.4\,M_\odot$, the total mass of stars formed (or to be formed) in CG 12 is found to be $\sim 50\,M_\odot$ (not counting any stars in the mass range 0.6–0.1 $M_\odot$ that may also form). The SFE will then be ∼33 per cent.

5 CONCLUSIONS

We have presented a photometric method to determine distances to dark clouds like Bok globules. In this method, we compute intrinsic colour indices of stars projected towards the direction of the cloud by dereddening the observed colour indices using various trial values of extinction A_V and a standard extinction law. These computed intrinsic colour indices for each star are then compared with the intrinsic colour indices of normal main-sequence stars and a spectral type is assigned to the star for which the computed colour indices best match with the standard intrinsic colour indices. Distances (d) to the stars are determined using the A_V and absolute magnitude (M_V) corresponding to the spectral types thus obtained. A distance versus extinction plot is made and the distance at which A_V undergoes a sharp rise is taken to be the distance to the cloud. The method has been demonstrated using CCD observations of fields containing the cometary globule CG 12. We have derived a distance of 550 pc to the cometary globule CG 12 from this method, which agrees more closely with the value derived by Williams et al. (1977) than with other estimates of its distance in the literature. The large distance to CG 12 makes this cloud an example of a site of high-mass star formation at relatively large height above the galactic plane. The efficiency of star formation in the cloud is estimated to be relatively high ($\gtrsim$16 per cent, to as large as ∼33 per cent). More recent radio maps confirm the existence of an H I shell centred at $l = 315^\circ$, $b = 30^\circ$, with CG 12 near its boundary and its tail pointing away from the centre of the shell. As suggested by Williams et al. (1977), a supernova explosion near the centre of the HI shell may have been responsible for the cometary morphology and for triggering star formation in CG 12 with a relatively high efficiency.

ACKNOWLEDGMENTS

This publication makes use of data products from the SIMBAD database, operated at CDS, Strasbourg, France and the Two Micron All Sky Survey, which is a joint project of the University of Massachusetts and the Infrared Processing and Analysis Center, funded by the National Aeronautics and Space Administration and the National Science Foundation. The optical image in Fig. 1, reproduced from the Digitized Sky Survey (DSS), is based on photographic data obtained using the UK Schmidt Telescope operated by the Royal Observatory Edinburgh, with funding from the UK Science and Engineering Research Council and the Anglo-Australian Observatory. The DSS was produced at the Space Telescope Science Institute under the US Government grant NAG W-2166. IRAF is distributed by National Optical Astronomy Observatories, USA. We thank the referee for critical comments and suggestions that have lead to improvements in the paper.

REFERENCES

Bahcall J. N., Soneira R. M., 1980, ApJS, 44, 73
Bhatt H. C., Maheswar G., Manoj P., 2004, MNRAS, 348, 83
Bok B. J., 1977, PASP, 89, 597
Bok B. J., Bok P. F., 1941, The Milky Way. Harvard Univ. Press, Cambridge, MA

Bok B. J., Reilly E. F., 1947, ApJ, 105, 255
Bourke T. L., Hyland A. R., Robinson G., 1995, MNRAS, 276, 1052
Brand P. W. J. L., Harwarden T. G., Longmore A. J., Williams P. M., Caldwell J. A. R., 1983, MNRAS, 203, 215
Carpenter J. M., 2001, AJ, 121, 2851
Cleary M. N., Haslam C. G. T., Heiles C., 1979, A&AS, 36, 95
Clemens D. P., Yun J. Lin., Heyer M. H., 1991, ApJS, 75, 877
Cutri R. M. et al., 2000, 2MASS All-Sky Catalog of Point Sources
Dickey J. M., Lockman F. J., 1990, ARA&A, 28, 215
Goss W. M., Manchester R. N., Brooks J. W., Sinclair M. W., Manefield G. A., Danziger I. J., 1980, MNRAS, 191, 533
Hawarden T. G., Brand P. W. J. L., 1976, MNRAS, 175, 19
Heiles C., 1976, ApJ, 208, L137
Herbst W., Sawyer D. L., 1981, ApJ, 243
Hobbs L. M., Blitz L., Magnani L., 1986, ApJ, 306, L109
Hog E. et al., 2000, A&A, 355, L27
Jacoby G. H., Hunter D. A., Christian C. A., 1984, ApJS, 56, 257
Johnson H. L., 1966, ARA&A, 4, 193
Kandori R., Dobashi K., Uehara H., Sato F., Yanagisawa K., 2003, AJ, 126, 1888
Keto E. R., Myers P. C., 1986, ApJ, 304, 466
Koornneef J., 1983, A&AS, 51, 489
Lada C. J., Lada E. A., 2003, ARA&A, 41, 57
Magnani L., Blitz L., Mundy L., 1985, ApJ, 295, 402
Maheswar G., Manoj P., Bhatt H. C., 2002, Bull. Astron. Soc. India, 30, 651
Marraco H. G., Forte J. C., 1978, ApJ, 224, 473
Mathis J. S., 1990, ARA&A, 28, 37
Otrupcek R. E., Hartley M., Wang J.-S., 2000, Publ. Astron. Soc. Aust., 17, 92
Peterson D. E., Clemens D. P., 1998, AJ, 116, 881
Prabhu T. P., Anupama G. C., Surendiranath R., 1998, Bull. Astron. Soc. India, 26, 383
Reed B. C., 2000, AJ, 120, 314
Reipurth B., 1983, A&A, 117, 183
Santos N. C., Yun J. L., Santos C. A., Marreiros R. G., 1998, AJ, 116, 1376
Schmidt-Kaler Th., 1982, in Schaifers K., Voigt H. H., eds, Landolt-Börnstein Numerical data and Functional Relationships in Science and Technology, New Series, Group VI, vol. 2(b). Springer-Verlag, Berlin, p. 1
Thé P. S., Tjin H. R. E., Steenman H., Wesselius P. R., 1986, A&A, 155, 347
van Hill H., Loren R., Davis J., 1975, ApJ, 198, 235
Vrba F. J., Rydgren A. E., 1984, ApJ, 283, 123
White G. J., 1993, A&A, 274, L33
Whittet D. C. B., 2003, Dust in the galactic environment, 2nd edn. IOP Publishing, Bristol
Whittet D. C. B., Kirrane T.M., Kilkenny D., Oates A. P., Watson F. G., King D. J., 1987, MNRAS, 224, 497
Williams P. M., Brand P. W. J. L., Longmore A. J., Hawarden T. G., 1977, MNRAS, 181, 709
Wolf M., 1923, Astron. Nachr., 219, 109
Yonekura Y., Hayakawa T., Mizuno N., Mine Y., Mizuno A., Ogawa H., Fukui Y., 1999, PASJ, 51, 837
Yun J. L., Clemens D. P., 1990, ApJ, 365, 73
Zealey W. J., Ninkov Z., Rice E., Hartley M., Tritton S. B., 1983, Astrophys. Lett., 23, 119

This paper has been typeset from a TEX/LATEX file prepared by the author.